ORIGINAL PAPER

On improving tropical cyclone track forecasts using a scale-selective data assimilation approach: a case study

Zhijuan Lai · Sai Hao · Shiqiu Peng · Bei Liu · Xiangqian Gu · Yu-Kun Qian

Abstract   A dynamical downscaling approach based on scale-selective data assimilation (SSDA) is applied to tropical cyclone (TC) track forecasts. The results from a case study of super Typhoon Megi (2010) show that the SSDA approach is very effective in improving the TC track forecasts by fitting the large-scale wind field from the regional model to that from the global forecast system (GFS) forecasts while allowing the small-scale circulation to develop freely in the regional model. A comparison to the conventional spectral-nudging four-dimensional data assimilation (FDDA) indicates that the SSDA approach outperforms the FDDA in TC track forecasts because the former allows the small-scale features in a regional model to develop more freely than the latter due to different techniques used. In addition, a number of numerical experiments are performed to investigate the sensitivity of SSDA's effect in TC track forecasts to some parameters in SSDA, including the cutoff wave number, the vertical layers of the atmosphere being adjusted, and the interval of SSDA implementation. The results show that the improvements are sensitive in different extent to the above three parameters.

Z. Lai · S. Peng (✉) · Y.-K. Qian
State Key Laboratory of Tropical Oceanography, South China Sea Institute of Oceanology, Chinese Academy of Sciences, Guangzhou 510301, China
e-mail: speng@scsio.ac.cn

Z. Lai · S. Hao
University of Chinese Academy of Sciences, Beijing 100049, China

S. Hao
LASG, Institute of Atmospheric Physics, Chinese Academy of Sciences, Beijing 100029, China

B. Liu
Institute of Ocean and Meteorology, Guangdong Ocean University, Zhanjiang 524088, China

X. Gu
State Key Laboratory of Sever Weather, Chinese Academy of Meteorological Sciences, Beijing 100081, China

1 Introduction

As one of the most destructive natural disasters, tropical cyclones (TC) have always been
paid much attention to by scientists. An accurate forecast of TC track and its landfall is a
prerequisite for preventing and mitigating TC-induced disasters, and thus is one of the most
important tasks in weather forecasting. Though steady improvements have been made over
the past several decades (Goerss et al. 2004; Cangialosi and Franklin 2011; Yu et al. 2012),
considerable track forecast errors still exist. For example, during the years from 2007 to
2011, the mean typhoon track forecast errors in the National Meteorological Center (CMA)
are 114, 190, and 287 km for 24, 48, and 72 h forecasts, respectively (Qian et al. 2012).
Therefore, TC track forecasting still remains a significant challenge to the forecasters all
over the world.

Because large-scale environmental flow is one of the important factors of TC motion
(Harr and Elsberry 1991; Carr and Elsberry 2000), the accuracy of TC track forecasting is
strongly dependent on that of the forecasting of large-scale environmental circulations.
Global models can describe large-scale features well and usually are considered to be a
good guidance for TC track forecasting. However, they are unable to satisfactorily resolve
regional-scale features due to relatively coarse resolution, generally resulting in an
underestimate of TC intensity. Regional models can better represent small-scale processes
due to their finer grid resolution than global models and thus can better simulate TC
intensity. Traditionally, the large-scale information from a global model is passed to a
regional model either through a sponge zone near lateral boundaries using a relaxation
procedure (Davies 1976), or through the so-called dynamical downscaling using spectral/
grid nudging techniques (Stauffer and Seaman 1990, 1994; Waldron et al. 1996; von Storch
et al. 2000; Castro et al. 2005; Deng and Stauffer 2006) or perturbation filter methods
(Hoyer 1987; Juang and Kanamitsu 1994). However, the large-scale information trans-
ferred through the lateral boundaries may be limited or distorted due to wave reflection
(Davies 1983) and that transferred by the conventional dynamical downscaling technique
could result in dynamical/physical inconsistency between the nudged variables and the
non-nudged variables in the model.

To overcome these shortcomings, Peng et al. (2010) proposed a dynamically consistent
method, referred to as scale-selective data assimilation (SSDA) approach, to correct the
large-scale bias by incorporating the large-scale circulations from a global model into a
regional model while keeping the regional-scale details unchanged. This SSDA approach
employs a band-pass digital filter and a three-dimensional variational data assimilation
(3DVAR) scheme. Studies have shown that the large-scale components from the global
analysis can be effectively assimilated into the regional model by SSDA approach,
resulting in an improvement of precipitation hindcast and TC track/intensity simulation in
an overall assessment (Peng et al. 2010; Xie et al. 2010; Liu and Xie 2012). However, as
mentioned by Peng et al. (2010), there are still considerable uncertainties in presetting the
values of some parameters in SSDA. These parameters include the cutoff wave number,
the vertical layers of the atmosphere being adjusted for a specific domain and its horizontal
resolution, and the interval of SSDA implementation. Therefore, it is necessary to

investigate the sensitivity of SSDA's performance to these parameters so that some practical guideline can be provided for the application of SSDA in operational forecasting in the future. Moreover, though a comparison between SSDA and the conventional analysis-nudging four-dimensional data assimilation (FDDA) (Stauffer and Seaman 1990, 1994; Castro et al. 2005; Deng and Stauffer 2006) was made by Xie et al. (2010) regarding their performance in TC track/intensity simulation, it was only based on a pair of experiments which were initialized at a single time in the context of hindcasting with the GFS analyses as the boundary conditions and the assimilated large-scale information. Thus, a more robust comparison between SSDA and spectral-nudging FDDA is still needed through a set of forecasts initialized at different time using GFS forecasts for the boundary conditions and data assimilation.

The rest of this paper is organized as follows. Section 2 gives a detailed description of the SSDA approach and the regional model used in this study. The data, model settings, and experiments design are described in Sect. 3. Section 4 presents the results and discussion, followed by summaries in Sect. 5.

2 The regional model and the SSDA approach

The version 3.2 of the Weather Research and Forecasting (WRF) system is employed in this study. The WRF, developed by National Center for the Atmosphere Research (NCAR), features a fully compressible, Eulerian non-hydrostatic control equation set, a terrain-following, hydrostatic pressure vertical coordinate system with the top of the model being a constant pressure surface, a horizontal Arakawa-C grid, Runge–Kutta 2nd- and 3rd-order time integration schemes, and 2nd–6th-order advection schemes. It incorporates various physical processes including microphysics, cumulus parameterization, planetary boundary layer (PBL), surface layer, land surface, and longwave and shortwave radiations, with several options available for each process. For more details, readers are referred to Wang et al. (2010).

The SSDA approach presented by Peng et al. (2010) is employed to assimilate the large-scale components of the circulation from the global model forecasts into the regional model WRF for TC track forecasts. The SSDA involves a low-pass filter and a 3DVAR technique from the WRF's data assimilation (WRFDA).The low-pass filter in SSDA is used to perform the scale separation of the forecasting (or analysis) fields from the global model or the regional model. It employs the discrete fast Fourier transform (FFT) together with a detrending program to deal with aperiodic lateral boundary. The large-scale components of the global model fields are assimilated into regional model to adjust the corresponding large-scale components using WRFDA. WRFDA is based on an incremental variational data assimilation technique and uses the conjugate gradient method to minimize the cost function in analysis control variable space.

The large-scale components of the global model fields are assimilated into the regional model at a preset time interval (i.e., the interval of SSDA implementation) as the model integration advances in time, as schematically illustrated in Fig. 1a with an example of 12-h interval of SSDA implementation. Figure 1b depicts the procedure of the SSDA approach. The entire procedure can be described briefly as follows: (1) A low-pass filter is used to separate fields from the regional model restart file (WRFRST) and the global forecast system (GFS) into large-scale components (LWRF and LGFS, respectively) and small-scale components (SWRF and SGFS, respectively) as the model integration reaches the time for inclusion of large-scale information from global models; (2) the large-scale

components obtained from the global model analyses or forecasts (LGFS) are assimilated into the corresponding components from the regional model (LWRF) using a 3DVAR approach; (3) the small-scale components from the regional model (SWRF obtained in step 1) and the updated large-scale components (ALWRF obtained in step 2) are combined to obtain the new full-scale circulation (NEWRST); and (4) integrating the regional model to the next time of SSDA implementation.

3 Experiment setup

Super Typhoon Megi (2010) was chosen for our experiments in this study. It caused great adverse impact on the safety of life and property in southeastern China. After generating over the ocean east off Philippines at 1200 UTC 13 Oct 2010, Typhoon Megi moved westward into the South China Sea and suddenly made a nearly 90-degree turn to the north around 0000 UTC 20 Oct and finally made a landfall at the coast of Fujian, China. The sudden track change posed major challenges to operational forecasters. As one of the most sophisticated, reliable, and accurate operational NWP models, the ECMWF model is highly respected and utilized by operational forecasters. Its ensemble forecast initialized from 0000 UTC 17 Oct to 0000 UTC 19 Oct exhibited dramatic divergence, representing great uncertainty in the future track of Megi (Qian et al. 2013). While some members predicted the storm to continue to move westward or northwestward, others predicted the storm to turn to the north. Additionally, the deterministic forecast differs significantly from the ensemble mean. Nearly, all of the CMA, JTWC, and JMA official 5-day track forecasts issued in these 2 days overpredicted the westward motion (Qian et al. 2012).

The real-time GFS global data from NCEP on $1.0° \times 1.0°$ global grids, which include analysis data at the initial time and 384-h forecasts, were updated every 6 h and are used to
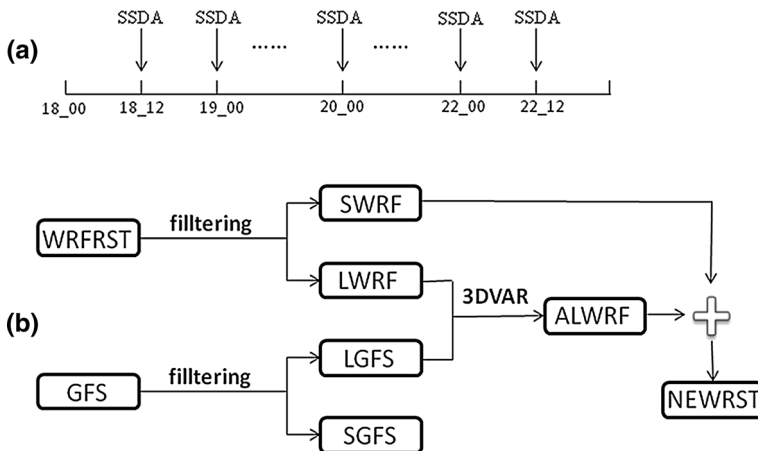

Fig. 1 Diagrams schematically illustrating **a** the SSDA implementation with an interval of 12 h during a 5-day forecast period starting at 0000 UTC 18 Oct 2010 (SSDA_REF) and **b** the procedure of the SSDA approach. Here, WRFRST and GFS denote the output from WRF (restart file) and the global forecast system (GFS), respectively; *SWRF* (*SGFS*) and *LWRF* (*LGFS*) denote the small-scale component and the large-scale component of the WRF (GFS) output, respectively; *ALWRF* denotes the adjusted LWRF after the assimilation of LGFS using 3DVAR approach; *NEWRST* denotes the new WRF restart file after a combination of SWRF and ALWRF
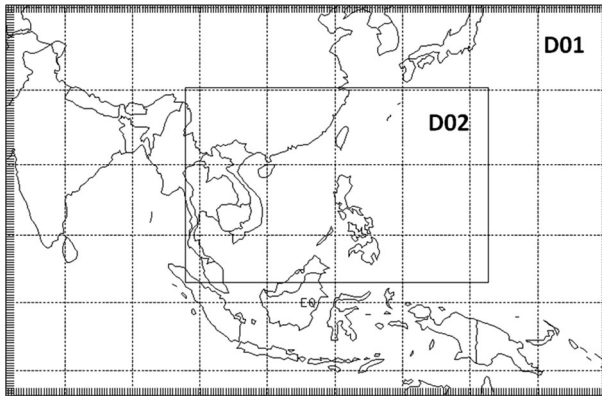
Fig. 2 Configuration of the model domains for all experiments

provide the initial conditions and boundary conditions as well as the large-scale information of the atmosphere required for the SSDA approach. In addition, the NCEP GFS global analyses and tropical cyclone best track data (also called OBS hereafter) from the Joint Typhoon Warning Center (JTWC) are used to validate the regional model simulation results.

The WRF model is configured with two nested domains centered at 15°N, 116°E in a Mercator map projection and 27 sigma levels in the vertical with the top of 50 hPa (see in Fig. 2). The outer and the inner domains cover 240 × 156 horizontal grid points with a grid spacing of 36 km (i.e., 8,604 km × 5,580 km) and 361 × 232 horizontal grid points with a grid spacing of 12 km (i.e., 4,320 km × 2,772 km), respectively. The integration time step for the outer domain is 180 s. The Ferrier (new Eta) microphysics scheme (Ferrier et al. 2002), the Kain–Fritsch cumulus scheme (Kain and Fritsch 1990), the Bougeault and Lacarrere (BouLac) TKE PBL scheme (Bougeault and Lacarrère 1989), and the Dudhia shortwave (Dudhia 1989) and rapid radiative transfer model (RRTM) longwave (Mlawer et al. 1997) radiation scheme are chosen in this study.

To make an overall assessment for the effect of the SSDA approach, we first perform a set of SSDA experiments that includes 9 runs of 5-day forecast initialized every 6 h from 0000 UTC 17 Sep 2010 to 0000 UTC 19 Sep 2010 and compare the results with those of the control experiments (without data assimilation, denoted as CTL) and the FDDA experiments. For the SSDA experiments, the wind components with wavelength longer than 2,151 km (corresponding to a cutoff wave number of four) at all sigma levels from the GFS forecasts are assimilated into the outer domain of the regional model at an interval of 12 h using 3DVAR technique as forecasting advances (as schematically indicated in Fig. 1a). The FDDA is a conventional data-digested approach using the grid or spectral-nudging technique (Stauffer and Seaman 1990, 1994; Waldron et al. 1996; von Storch et al. 2000; Deng and Stauffer 2006), which is built in the standard WRF package. Spectral-nudging technique has been employed in some studies associated with seasonal TC simulations or individual typhoon case study (Knutson et al. 2007; Feser and von Storch 2008a, b) to constrain the large-scale circulation in the regional model domain interior to that from the global analyses or forecasts while allowing the small-scale dynamics of the regional model to develop. To be comparable to the SSDA experiments, here the spectral-nudging scheme is employed to digest the large-scale wind field with wavelength longer

than 2,151 km (by setting xwavenum = 4 in the scheme, where xwavenum is the parameter of the x-direction wave number) at all sigma levels from GFS forecasts into the regional model. The analysis interval and the last analysis time are 6 and 114 h, respectively. By tuning the parameters of spectral nudging for a best performance, the nudging coefficient of 0.0003 (corresponding to a relaxation time of 56 min, or about 1 h) is adopted, and the nudging is ramped for a period of 60 min (staring from hour 114 and ending at hour 115). It should be noted that although both SSDA and FDDA fit the large-scale wind field from the regional model to that from the global model, the techniques used in the two methods are different. SSDA employs a 3DVAR technique in which the non-assimilated variables (i.e., other variables except wind field in this study) are adjusted directly through the cross correlation between different meteorological fields prescribed in the background error covariance, while FDDA uses a spectral-nudging technique in which the non-nudged variables are adjusted indirectly through the dynamic constraint during the model integration. The experiments initialized at 0000 UTC 18 Oct 2010 are selected for a detailed analysis and comparison among CTL, SSDA, and FDDA.

To investigate the sensitivity of the SSDA approach to the cutoff wave number (denoted as "CWN"), the vertical layers of the atmosphere being adjusted (denoted as "VLA"), and the interval of SSDA implementation (denoted as "INT"), three sets of experiments (see Table 1) are designed. Each type of experiments in each set includes 9 runs of 3-day forecast initialized every 6 h from 0000 UTC 17 Sep 2010 to 0000 UTC 19 Sep 2010 (we denote this "9 runs" as an "ensemble" hereafter). The "ensemble" of SSDA experiments, in which the wind fields with wavelength longer than 2,151 km (corresponding to CWN = 4) at levels about 800–100 hPa from the GFS forecasts are assimilated into the regional model at an interval of 12 h, is taken as a reference and denoted as SSDA_REF in the three sets of sensitivity experiments. The first set of experiments aims to investigate the sensitivity of SSDA to the CWN. It consists of five SSDA "ensembles" (denoted as SSDA1w, SSDA2w, SSDA3w, SSDA5w, and SSDA6w, respectively), which are the same as SSDA_REF except that they employ a different CWN of one, two, three, five, and six (corresponding to a wavelength of 8,604, 4,302, 2,868, 1,720.8, and 1,434 km for the model domain, respectively). The second set of experiments is designed to investigate the sensitivity of SSDA to the VLA. It includes four SSDA "ensembles" (denoted as SSDA500, SSDA700, SSDA900, SSDAall), which are the same as SSDA_REF except that they adjust different vertical layers of approximately 500–100, 700–100, 900–100, and 1,000–50 hPa, respectively. The last set of experiments aims to test the sensitivity of SSDA to the INT during the forecasting period. It includes three SSDA "ensembles" (denoted as SSDA3h, SSDA6h, and SSDA24h, respectively), which are the same as SSDA_REF except that they employ a different INT of 3, 6, and 24 h, respectively.

4 Results and discussion

The TC tracks forecast by all sets of experiments are compared with the JTWC tropical cyclone best track data ("observations") and NCEP GFS global analyses. In this study, the TC center is defined as the location of the minimum sea level pressure, and the track position error (TPE in km) is defined as the great circle distance between the "observed" TC center and the forecast one valid at the same time, which can be calculated by the following formulas (Neumann and Pelissier 1981; Powell and Aberson 2001):

Table 1 Sensitivity experiments designed in the study

Sets of exp.	Exp. name	Cutoff wave number (CWN)	Interval of SSDA implementation (INT)	Vertical layers of atmosphere being adjusted (VLA)
Ref. exp.	SSDA_REF	4 ($\sim$2,151 km)	12 h	Sigma levels between 7th and 24th ($\sim$800–100 hPa)
1st	SSDA1w	1 ($\sim$8,604 km)	12 h	Sigma levels between 7th and 24th ($\sim$800–100 hPa)
	SSDA2w	2 ($\sim$4,302 km)	As above	As above
	SSDA3w	3 ($\sim$2,868 km)	As above	As above
	SSDA5w	5 ($\sim$1,720.8 km)	As above	As above
	SSDA6w	6 ($\sim$1,434 km)	As above	As above
2nd	SSDA500	4 ($\sim$2,151 km)	12 h	Sigma levels between 13th and 24th ($\sim$500–100 hPa)
	SSDA700	As above	As above	Sigma levels between 9th and 24th ($\sim$700–100 hPa)
	SSDA900	As above	As above	Sigma levels between 7th and 24th ($\sim$900–100 hPa)
	SSDAall	As above	As above	Sigma levels between 1th and 27th (1,000–50 hPa)
3rd	SSDA3h	4 ($\sim$2,151 km)	3 h	Sigma levels between 7th and 24th ($\sim$800–100 hPa)
	SSDA6h	As above	6 h	As above
	SSDA24h	As above	24 h	As above

$$TPE = 111.11 \cos^{-1}[\sin \varphi_0 \sin \varphi_f + \cos \varphi_0 \cos \varphi_f \cos(\lambda_0 - \lambda_f)],$$

where φ_0 and λ_0 are the latitude and longitude of the "observed" TC center, and φ_f and λ_f are the latitude and longitude of the forecast TC center.

4.1 Effects of the SSDA approach on TC track forecasts

Table 2 presents the mean track forecast errors at different forecast periods for the CTL, FDDA, and SSDA runs. The results from GFS global forecasts and JTWC forecasts are also given for comparison. The mean track forecast errors for different forecast periods from SSDA, CTL, FDDA, and GFS are much smaller than those from the JTWC forecasts. The SSDA performs the best with a mean TPE of 135.7 km, compared to those of 237.0 km for the control, 183.7 km for FDDA, and 179.9 km for the GFS. The GFS has a much smaller mean TPE than the CTL, implying that the large-scale environmental flows are better represented in the former than in the latter. Though both SSDA and FDDA fit the large-scale wind field of the regional model to that of the GFS forecasts, the improvement of track forecast for SSDA is larger than that for FDDA. The reason could be that SSDA allows the regional-scale circulation to develop more freely in the regional model than FDDA by using a 3DVAR technique which is of multivariable adjustment. Moreover, it is worth noting that the TPEs from SSDA are smaller than those from GFS, which implies that the improvements of track forecasting in SSDA are not bounded by the assimilated large-scale circulation from GFS. This could be attributed to microphysics included in the regional model as well as the nonlinear interactions between the improved large-scale components and the freely developed small-scale components of circulation in SSDA,

Table 2 Mean track forecast errors at different forecast periods for the CTL, FDDA, and SSDA runs, as well as the JTWC and GFS global forecasts (unit: km)

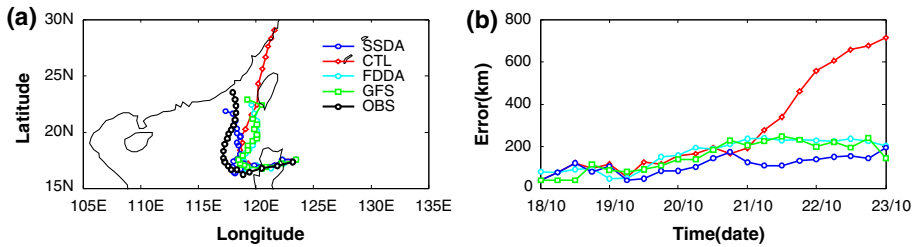| Expt.	Forecast period (h) and (no. of cases)					
	24 (9)	48 (9)	72 (9)	96 (9)	120 (9)	Mean
CTL	70.6	132.3	190.0	333.6	458.3	237.0
FDDA	71.2	138.7	187.6	229.6	291.5	183.7
SSDA	63.3	95.3	119.1	151.9	248.8	135.7
GFS	73.2	130.1	178.0	238.5	279.9	179.9
JTWC	81.6	150.4	318.3	541.0	713.2	360.9

Fig. 3 Forecast **a** TC track and **b** corresponding errors (unit: km) for experiments CTL (in *red*), SSDA (in *blue*), and FDDA (in *cyan*), and the GFS global forecasts (in *green*), initialized at 0000 UTC 18 Oct 2010. The JTWC best track data (OBS, in *black*) is also given as reference

Table 3 Track forecast errors for experiments CTL, FDDA, and SSDA, and the GFS global forecasts, initialized at 0000 UTC 18 Oct 2010 (unit: km)

	Track errors (km)			
	CTL	FDDA	SSDA	GFS
3-Day mean	131.4	131.4	98.2	121.2
5-Day mean	293.1	169.5	115.3	157.7

which will be seen in the following analysis. Therefore, we conclude that the SSDA approach is an effective means of improving TC track forecasts and better than the conventional approach FDDA.

To see more clearly the performance of the SSDA approach, we make a detailed analysis on the results from the experiments initialized at 0000 UTC 18 Oct. Figure 3 shows the forecast TC tracks and corresponding errors for experiments CTL, SSDA, and FDDA, and the GFS global forecasts. It is clear that SSDA performs better than CTL, FDDA, and GFS in track forecast, especially for forecast period longer than 72 h. The TC forecast by CTL moves much faster and deviates to the east compared to the observed one, and that forecast by the GFS moves slower than CTL but still deviates to the east. The TC forecast by FDDA follows that by GFS, while that by SSDA cannot only slowdown but also steer westward to be closer to the observed one, leading to the smallest mean TPE. The 3-day and 5-day mean TPEs decrease from 131.4 and 293.1 km for CTL to 98.2 and
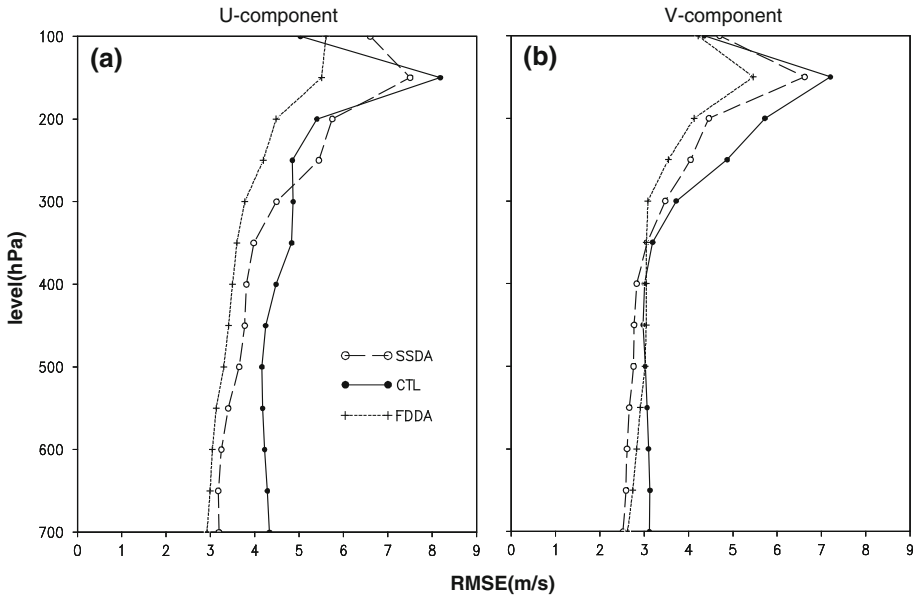
Fig. 4 Vertical profiles of 5-day mean RMSEs for large-scale **a** u and **b** v components against GFS analysis for experiments CTL, SSDA, and FDDA, initialized at 0000 UTC 18 Oct 2010. The RMSEs are averaged over all grids in the inner domain (unit: m s^{-1})

115.3 km for SSDA, respectively, as shown in Table 3. Figure 4 shows the vertical profiles of 5-day mean root-mean-square errors (RMSEs) of the large-scale u and v components for the SSDA and FDDA against the GFS analysis averaged over all grids in the inner domain. Both SSDA and FDDA have significant reduction in the RMSEs of the large-scale wind components nearly at all vertical levels above 700 hPa compared to the control run, with FDDA having the smallest RMSEs in the u component. However, the smallest RMSEs of the large-scale circulation in the regional model against the GFS analysis do not necessarily lead to a best track forecast for a TC, because the movement of a TC can be influenced by environmental systems of different scales (Chen and Luo 1995b; Zhu 1996; Meng et al. 2002). Figure 5 gives the 700-hPa wind fields before the track turning time for experiments CTL, SSDA, and FDDA initialized at 0000 UTC 18 Oct. It is clear that the FDDA experiment produced a much weaker TC than the CTL and SSDA experiments. As shown in Chen and Luo (1995a), the asymmetric structure of the inner core of a tropical cyclone could influence its movements. In Fig. 5, the area of the enhanced winds at 700-hPa for the SSDA experiment shifts clockwise at 0000 UTC 20 Oct (right before the observed track turning time), which is in agreement with Wu et al. (2013) who suggested that the sudden track changes are closely related to the evolution of asymmetric wind patterns at the low levels, i.e., a clockwise (counterclockwise) enhanced winds shift prior to the track turning is corresponding to a north-turning (west-turning) of a TC. For CTL, however, the clockwise shift of the area of the enhanced winds occurs at an earlier time (1,200 UTC 19 Oct), which may cause the forecast TC to turn north earlier and deviate to the east compared to the observed one. This implies that the assimilation of large-scale flows from the GFS global forecasts by the SSDA approach may be not only effective in improving the simulation of the large-scale circulation but also beneficial to represent the small-scale features in the regional model, leading to significant improvements in TC track
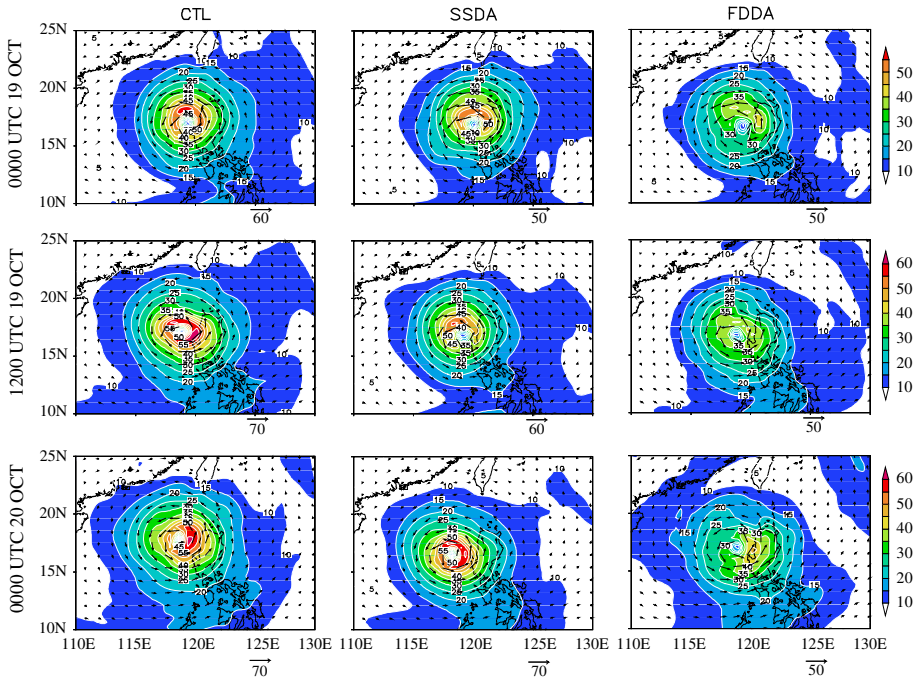
Fig. 5 700-hPa wind (vectors) and its magnitude (shading and contours, unit: m s^{-1}) for experiments CTL, SSDA, and FDDA, initialized at 0000 UTC 18 Oct 2010
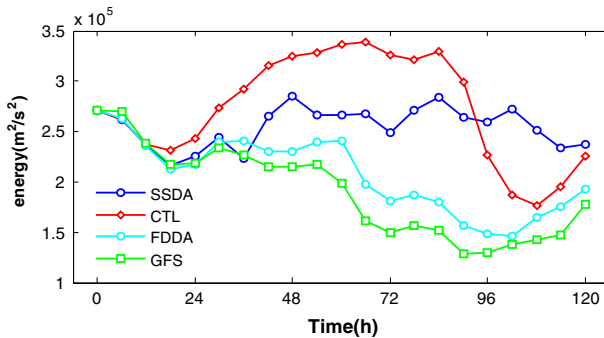

Fig. 6 Temporal evolution of the small-scale kinetic energy (unit: m^2 s^{-2}) for experiments CTL, SSDA, and FDDA, and the GFS global forecasts, initialized at 0000 UTC 18 Oct 2010

forecasts. Figure 6 displays the temporal evolution of the small-scale kinetic energy for different experiments. It is found that the small-scale features in the regional model are well developed in the SSDA experiment compared with those in the FDDA one when fitting the large-scale wind component of the regional model to that of the GFS forecasts, which could be caused by the different techniques used in these two methods, including spectral filtering techniques and data digesting techniques.

According to the above discussion, by fitting the large-scale flows from the regional model to those from the GFS global forecasts, both FDDA and SSDA approaches are able

Fig. 7 Mean track position errors (unit: km) for SSDA experiments with different cutoff wave numbers at different forecast periods
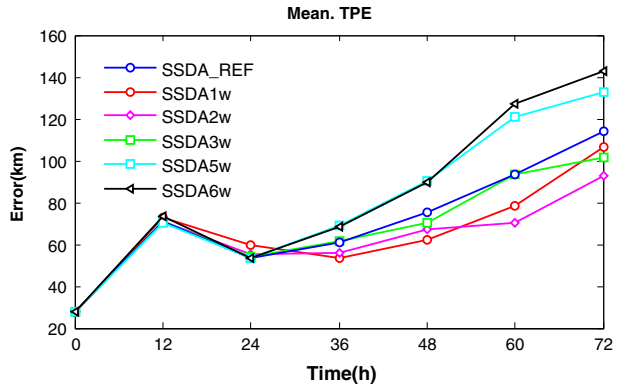

Table 4 Mean track forecast errors at different forecast periods for SSDA experiments with different cutoff wave numbers (unit: km)

Expt.	Forecast period (h) and (no. of cases)						
	12 (9)	24 (9)	36 (9)	48 (9)	60 (9)	72 (9)	Mean
SSDA_REF	71.1	53.6	61.2	75.5	93.5	113.9	78.1
SSDA1w	71.1	59.7	53.5	62.4	78.3	106.5	71.9
SSDA2w	71.1	55.3	55.6	67.5	70.3	92.6	68.7
SSDA3w	71.1	54.3	61.7	70	93.4	101.7	75.4
SSDA5w	71.1	53.2	69	90.2	121.1	132.9	89.6
SSDA6w	71.1	53.1	68.5	89.6	127	142.6	92.0

to improve TC track forecasts effectively. But due to different techniques used, the development of the small-scale features in the regional model is constrained severely by the FDDA approach, while the small-scale features in the regional model are well developed by the SSDA approach, which results in the best TC track forecasts in the SSDA experiments.

4.2 Sensitivity of the SSDA approach to CWN, VLA, and INT

In the first set of experiments, different CWNs are chosen to investigate the sensitivity of SSDA's effect to the parameter. It can be seen that the TC track can be influenced considerably by the CWN in SSDA approach. Tracks forecast by experiments with larger CWN deviates to east of the best track (not shown). The mean track forecast errors for the "ensemble" SSDA experiments with different CWNs at different forecast periods are presented in Fig. 7. It can be seen that the TC track forecast errors vary with the CWNs in SSDA approach. In general, the track forecast errors for experiments with smaller CWNs are smaller than those for experiments with larger CWNs during the 3-day forecast. On the overall estimate, experiments with CWN of 2 (SSDA2w, corresponding to a wavelength of 4,302 km) perform the best during the 3-day forecast with a mean TPE of 68.7 km (Table 4). The vertical profiles of 3-day mean RMSEs of the large-scale u and v
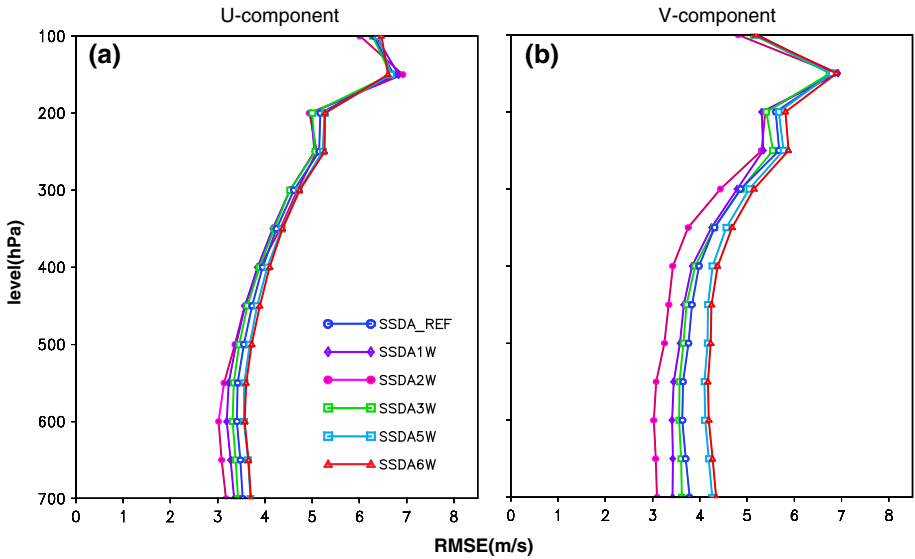
Fig. 8 Vertical profiles of 3-day mean RMSEs for large-scale **a** u and **b** v components against GFS analysis for the SSDA experiments with different cutoff wave numbers, initialized at 0000 UTC 18 Oct 2010. The RMSEs are averaged over all grids in the inner domain (unit: m s^{-1})

Fig. 9 Mean track position errors (unit: km) at different forecast periods for SSDA experiments with different vertical layers of the large-scale atmosphere being adjusted
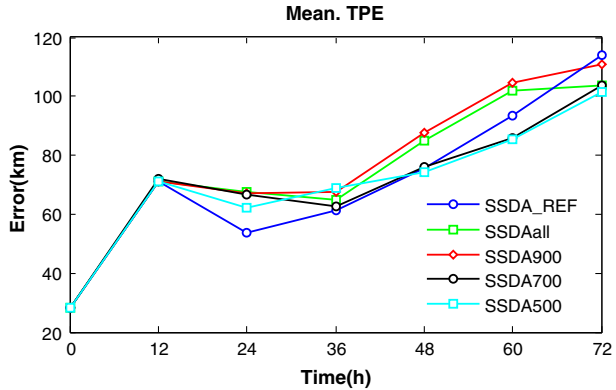
components against the GFS analysis for the SSDA experiments initialized at 0000 UTC 18 Oct are shown in Fig. 8. The SSDA2w has the smallest RMSEs of the large-scale flows fitting in these 3 days, resulting in a best track forecast.

The mean track forecast errors at different forecast periods for experiments with different VLAs are shown in Fig. 9. It is found that the track forecast errors only vary slightly with different VLAs during the 3-day forecast with a small range of 77.2–82.3 km (Table 5). As indicated in Table 5, the SSDA500 performs the best with a mean TPE of 77.2 km during the 3-day forecast. This is in agreement with the fact that the mid- to upper levels of the atmosphere are predominated by larger-scale circulation, and the small-scale

Table 5 Mean track forecast errors at different forecast periods for SSDA experiments with different vertical layers being adjusted (unit: km)

Expt.	Forecast period (h) and (no. of cases)						
	12 (9)	24 (9)	36 (9)	48 (9)	60 (9)	72 (9)	Mean
SSDA_REF	71.1	53.6	61.2	75.5	93.5	113.9	78.1
SSDAall	71.1	67.4	65.1	84.7	101.8	103.9	82.3
SSDA900	71.1	67.3	67.6	87.8	104.5	110.8	84.9
SSDA700	71.1	66.8	62.7	75.9	85.9	103.8	77.7
SSDA500	71.1	62.2	68.9	74.3	85.2	101.3	77.2

Fig. 10 Mean track position errors (unit: km) at different forecast periods for SSDA experiments with different interval of SSDA implementation
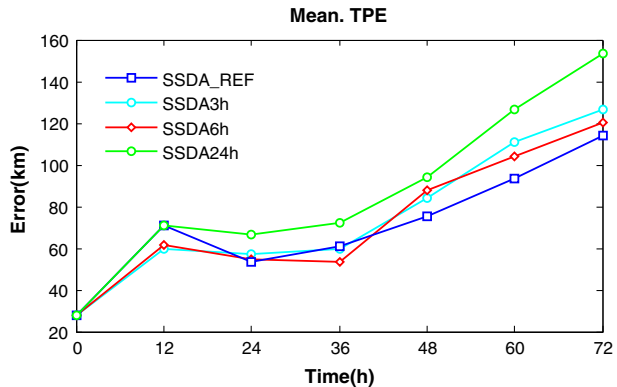
Table 6 Mean track forecast errors at different forecast periods for SSDA experiments with different interval of SSDA implementation (unit: km)

Expt.	Forecast period (h) and (no. of cases)						
	12 (9)	24 (9)	36 (9)	48 (9)	60 (9)	72 (9)	Mean
SSDA_REF	71.1	53.6	61.2	75.5	93.5	113.9	78.1
SSDA3h	59.5	57.1	59.8	83.8	110.7	126.3	82.9
SSDA6h	61.4	54.9	53.7	87.6	104.1	120.5	80.4
SSDA24h	71.2	66.8	72	93.8	126.5	153.3	97.2

Table 7 Mean track forecast errors at different forecast periods for SSDA experiments with CWN = 2 (corresponding to a wavelength of about 4,302 km), VLA = 500–100 hPa, and INT = 12-h (unit: km)

Expt.	Forecast period (h) and (no. of cases)						
	12 (9)	24 (9)	36 (9)	48 (9)	60 (9)	72 (9)	Mean
2W500L12h	71.1	54.7	53.5	62.4	70.5	95.5	68.0

features mainly develop or originate near the surface and lower atmosphere (Giorgi and Mearns 1999).

The mean track forecast errors at different forecast periods from the third set of sensitivity experiments are presented in Fig. 10. It is clear that TC track forecasts are improved evidently with INT decreasing from 24 h (for SSDA24h) to 12 h (for SSDA_REF). It is also found that reducing INT from 12 to 6 or 3-h dose not results in further improvement of the typhoon track forecast. In general, the SSDA_REF performs the best with the smallest mean track errors during the 3-day forecast (Table 6).

According to the above results of sensitivity experiments, an "optimal" setup in SSDA implementation for the track forecast of Megi with CWN = 2, VLA = 500–100 hPa, and INT = 12-h is made, and a set of experiments with this "optimal" setup are performed, initializing every 6 h from 0000 UTC 17 Sep 2010 to 0000 UTC 19 Sep 2010. The mean track forecast errors at different forecast periods for this set of experiments are given in Table 7. It can be seen that the "optimal" setup in SSDA produces the best track forecast with the smallest mean TPE of 68.0 km for the 3-day forecast.

5 Summaries

In this study, a number of experiments for super Typhoon Megi (2010) are performed to investigate the effect of the SSDA approach on TC track forecasts as well as its sensitivity to the cutoff wave number (CWN), the vertical layers of the atmosphere being adjusted (VLA), and the interval of SSDA implementation (INT). The experimental results show that the SSDA approach, benefiting from the merits of both global models in representing the large-scale environment flows and regional models in describing the small-scale features with high resolution, is able to improve TC track forecasts effectively, better than the spectral-nudging FDDA approach.

The effect of SSDA approach in TC track forecasts is dependent in different extent on the cutoff wave number (CWN), the vertical layers of the atmosphere being adjusted (VLA), and the interval of SSDA implementation (INT). For the domain designed in our case study of Megi, the SSDA approach performs the best in the track forecast with CWN = 2 (corresponding to a wavelength of about 4,302 km), VLA = 500–100 hPa, and INT = 12-h.

It is worth noting the sensitivity of the SSDA's effect in TC track forecasts to the parameters in SSDA discussed above may be case-dependent. In particular, the sensitivity of the SSDA's effect in TC track forecasts to the cutoff wave number may largely depend on the region and the model domain size. Therefore, more case studies regarding the sensitivity of SSDA's effect in TC track forecasts to the parameters discussed above are needed before the application of SSDA approach in operational TC forecasts, so that an "optimal" value of each parameter in an overall assessment is found for a specific region and model domain. Moreover, it should be also aware that the effect of SSDA in TC forecasts may greatly depend on the accuracy of the large-scale circulation from global models.

References

Bougeault P, Lacarrère P (1989) Parameterization of orography-induced turbulence in a mesobeta-scale model. Mon Weather Rev 117:1872–1890

Cangialosi JP, Franklin JL (2011) 2010 National Hurricane Center forecast verification report. NOAA, 77 pp. http://www.nhc.noaa.gov/verification/pdfs/verification_2010.pdf

Carr LE, Elsberry RL (2000) Dynamical tropical cyclone track forecast errors. Part II: Midlatitude circulation influences. Weather Forecast 15:662–681

Castro CL, Pielke Sr RA, Leoncini G (2005) Dynamical downscaling: assessment of value retained and added using the regional atmospheric modeling system (RAMS). J Geophys Res 110:D05108. doi:10.1029/2004JD004721

Chen L, Luo Z (1995a) Some relations between asymmetric structure and motion of typhoons. Acta Meteorol Sin 9(4):412–419

Chen L, Luo Z (1995b) Effect of the interaction of different-scale vortices on the structure and motion of typhoon. Adv Atmos Sci 12(2):207–214

Davies HC (1976) A lateral boundary formulation for multi-level prediction models. Q J R Meteorol Soc 102:405–418

Davies HC (1983) Limitations of some common lateral boundary schemes used in regional NWP models. Mon Weather Rev 111:1002–1012

Deng A, Stauffer DR (2006) On improving 4-km mesoscale model simulations. J Appl Meteorol Clim 45:361–381

Dudhia J (1989) Numerical study of convection observed during the winter monsoon experiment using a mesoscale two-dimensional model. J Atmos Sci 46:3077–3107

Ferrier BS, Jin Y, Lin Y, Black T, Rogers E, DiMego G (2002) Implementation of a new grid-scale cloud and precipitation scheme in the NCEP Eta model. Preprints. In: 19th conference on weather analysis and forecasting/15th conference on numerical weather prediction. American Meteorological Society, San Antonio, TX, pp 280–283

Feser F, von Storch H (2008a) A dynamical downscaling case study for typhoons in Southeast Asia using a regional climate model. Monthly Weather Rev 136:1806–1815

Feser F, von Storch H (2008b) Regional modelling of the western Pacific typhoon season 2004. Meteorol Z 17:519–528

Giorgi F, Mearns LO (1999) Introduction to special section: regional climate modeling revisited. J Geophys Res 104(D6):6335–6352

Goerss JS, Sampson CR, Gross JM (2004) A history of western North Pacific tropical cyclone track forecast skill. Weather Forecast 19:633–638

Harr PA, Elsberry RL (1991) Tropical cyclone track characteristics as a function of large-scale circulation anomalies. Monthly Weather Rev 119:1448–1468

Hoyer JM (1987) The ECMWF spectral limited area model. In: Proceedings of ECMWF workshop on techniques for horizontal discretization in numerical weather prediction models, Reading, United Kingdom, ECMWF, pp 343–359

Juang HMH, Kanamitsu M (1994) The NMC nested regional spectral model. Mon Weather Rev 122:3–26

Kain JS, Fritsch JM (1990) A one-dimensional entraining detraining plume model and its application in convective parameterization. J Atmos Sci 47:2784–2802

Knutson TR, Sirutis JJ, Garner ST, Held IM, Tuleya RE (2007) Simulation of the recent multidecadal increase of Atlantic hurricane activity using an 18-km-grid regional model. Bull Am Meteorol Soc 10:1549–1565

Liu B, Xie L (2012) A scale-selective data assimilation approach to improving tropical cyclone track and intensity forecasts in a limited-area model: a case study of Hurricane Felix (2007). Weather Forecast 27:124–140

Meng Z, Chen L, Xu X (2002) Recent progress on tropical cyclone research in China. Adv Atmos Sci 19:103–110

Mlawer EJ, Taubman SJ, Brown PD, Iacono MJ, Clough SA (1997) Radiative transfer for inhomogeneous atmosphere: RRTM, a validated correlated-k model for the longwave. J Geophys Res 102:16663–16682

Neumann CJ, Pelissier JM (1981) An analysis of Atlantic tropical cyclone forecast errors, 1970–1979. Mon Weather Rev 109:1248–1266

Peng S, Xie L, Liu B, Semazzi F (2010) Application of scale-selective data assimilation to regional climate modeling and prediction. Mon Weather Rev 138:1307–1318

Powell MD, Aberson SD (2001) Accuracy of United States tropical cyclone landfall forecasts in the Atlantic basin (1976–2000). Bull Am Meteorol Soc 82:2749–2767

Qian C, Duan Y, Ma S, Xu Y (2012) The current status and future development of China operational typhoon forecasting and its key technologies. Adv Meteorol Sci Technol 2(5):36–43

Qian C, Zhang F, Green BW (2013) Probabilistic evaluation of the dynamics and prediction of super Typhoon Megi (2010). Weather Forecast 28:1562–1577

Stauffer DR, Seaman NL (1990) Use of four-dimensional data assimilation in a limited-area mesoscale model. Part I: Experiments with synoptic-scale data. Mon Weather Rev 118:1250–1277

Stauffer DR, Seaman NL (1994) Multiscale four-dimensional data assimilation. J Appl Meteorol 33:416–434

von Storch H, Langenberg H, Feser F (2000) A spectral nudging technique for dynamical downscaling purposes. Mon Weather Rev 128:3664–3673

Waldron KM, Paegle J, Horel JD (1996) Sensitivity of a spectrally filtered and nudged limited-area model to outer model options. Mon Weather Rev 124:529–547

Wang W, Bruyere C, Duda M, Dudhia J, Gill D, Lin HC, Michalakes J, Rizvi S, Zhang X (2010) Advanced Research WRF (ARW) version 3 modeling system user's guide. ARW Tech Note

Wu L, Ni Z, Duan J, Zong H (2013) Sudden tropical cyclone track changes over the western North Pacific: a composite study. Mon Weather Rev 141:2597–2610

Xie L, Liu B, Peng S (2010) Application of scale-selective data assimilation to tropical cyclone track simulation. J Geophys Res 115:D17105. doi:10.1029/2009JD013471

Yu H, Chan ST, Brown B, Kunitsugu M, Fukada E, Park S, Lee W, Xu Y, Phalla P, Sysouphanthavong B, Chang SW, Ismall CG, Paciente RB, Ee P, Kaeochada C, Van HV (2012) Operational tropical cyclone forecast verification practice in the western North Pacific region. Trop Cyclone Res Rev 1:361–372

Zhu Y (1996) Numerical study of the influence of the large-scale basic flow speed variance on the tropical cyclone movement. Typhoon experiment and theoretical research II. China Meteorological Press, Beijing, pp 35–41 (in Chinese)